Vehicle-Detector Interactions and Analysis of Traffic-Actuated Signal Controls

FENG-BOR LIN and MARTIN C. PERCY

ABSTRACT

In modeling the queueing behavior of vehicles for analyzing traffic-actuated signal controls, existing simulation studies have treated only queue discharge headways explicitly. Other vehicle-detector interactions, which govern the initiation, extension, and termination of a green duration, are largely embedded in obscure algorithms for processing vehicles. This negligence has led to misleading and unrealistic findings. Based on data collected at three intersections in Syracuse, New York, some basic characteristics of vehicle-detector interactions that should be accounted for in simulating traffic-actuated controls are described. Further studies are needed to establish baseline information for examining the role of such interactions in shaping control efficiency and for calibrating simulation models.

Traffic-actuated signal controls commonly used today include semiactuated control, full-actuated control, and volume-density control. These controls are operated either on pulse mode with small-area, motion detectors or on presence mode with large-area detectors. One of the major problems in employing these controls lies in the determination of ways of achieving high control efficiencies. This problem is often dealt with through computer simulation analysis.

Existing simulation analyses of traffic-actuated signal controls appear to be very weak in modeling the interactions between queueing vehicles and detectors. These vehicle-detector interactions can be perceived to begin when a vehicle enters a detection area and to end when the vehicle moves downstream into an intersection. In a simulation analysis, usually only queue discharge headways have been treated explicitly. The way queueing vehicles actuate detectors is invariably buried in an embedded algorithm for processing vehicles. This lack of attention to such interactions has quite possibly led to incompatible or even unrealistic conclusions regarding the operating characteristics of traffic-actuated controls. Several existing analyses serve to underline this possibility.

In an analysis of pulse mode full-actuated control, Morris and Pak-poy (1) point out that, to minimize delays, vehicle interval should be reduced from about 8 seconds at an approach volume of 200 vehicles per hour (vph) to about 2 seconds at 800 vph. A study by Michalopoulos et al. (2) based on a UTCS-1 model (3) revealed a different operating characteristic for such a control. It showed that vehicle intervals of 2 sec resulted in better control efficiencies than longer ones for traffic volumes ranging from 200 to 700 vph per lane. Using the NETSIM model (4), Tarnoff and Parsonson (5) further found that vehicle intervals of 1 sec produced shortest delays for traffic volumes ranging from 200 to 1,500 vph per approach. In the same study they also examined presence mode full-actuated controls for detector lengths of 30, 60, and 90 ft. These lengths corresponded to extension intervals of 0.6, 1.2 and 1.8 sec under the simulated conditions. The analysis showed that delays decreased as detector length was shortened.

Something is obviously amiss in the results of these analyses. Queueing vehicles in a traffic lane often require more than 2 sec to reach and actuate a detector successively. When vehicle intervals of 1 or 2 sec are used, queueing vehicles may not have ample opportunities to actuate and extend green durations. Consequently, premature termination of a green duration may take place. Such an event is more likely to degrade the efficiency of a control than to improve it. Realizing this, Tarnoff and Parsonson cautioned that the simulation results should not be taken for granted.

Their caution deserves attention. Simulation is perhaps the only practical means of providing a comprehensive analysis of a signal control. Yet simulation based on unrealistic modeling of vehicle-detector interactions may result in misleading information. Grave consequences may follow if such information is unknowingly used as a basis for operating existing signal controls or for developing future generations of control.

In light of these possible implications, there is a need to identify the vehicle-detector interactions under traffic-actuated controls. In response to this need, a preliminary effort was made to collect relevant field data at three intersections in Syracuse, New York. The observed vehicle-detector interactions are described, and several basic requirements for simulating such interactions are identified.

DATA COLLECTION

When motion detectors are used, the operation of a control is dictated by the arrivals of vehicles at the detectors. These arrivals can be influenced by the detector setback that is denoted as L in Figure 1. If presence detectors are used instead, the arrivals of vehicles at the upstream edges of the detectors as well as the subsequent departures of the same vehicles from the downstream edges can affect the operation of the control. Therefore, the movement of a vehicle in relation to the detector length becomes an important factor. This detector length is also denoted as L in Figure 1.

Three sites in Syracuse, New York, were selected for data collection. These sites were the intersections between Almond Street and Harris Street, Almond Street and Adam Street, and Erie Boulevard and Kinne Avenue. At the first site, the queueing vehicles in three straight lanes on Almond Street were the subject of the data collection. At the second site, the movements of queueing vehicles in an exclusive left-turn lane on Almond Street were recorded. And, at the last site, the queueing vehi-

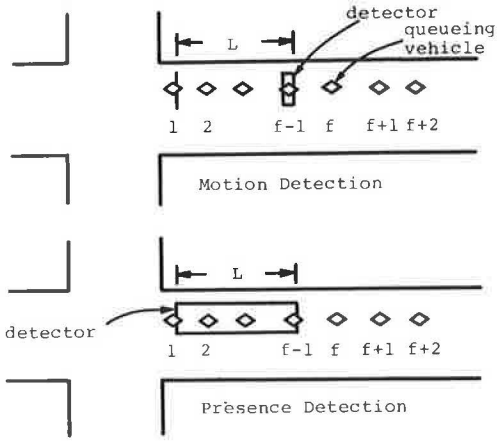

FIGURE 1 Detector placements for traffic-actuated control.

cles on an exclusive left-turn lane on Erie Boulevard were also included in the data collection.

At the three sites, parking was prohibited and pedestrian influences on the vehicular flows were virtually nonexistent. The approach speeds of the observed vehicles were generally between 30 and 35 mph. The flows in both selected left-turn lanes were characterized by a significant number of U-turns around curbed medians.

To facilitate data collection, hypothetical placements of detectors corresponding to detector setbacks or detector lengths of 30, 50, 80, and 120 ft were used. No distinctions were made between motion detection and presence detection. The reason for this is that data can be collected with respect to the same variable, L, as shown in Figure 1, in either case.

For each detector placement, two types of data concerning the movement of a queueing vehicle were recorded. One was the elapsed time from the onset of a green duration to the moment the front bumper of a queueing vehicle reached the upstream edge of the detector. This elapsed time will be referred to as arrival time for the sake of convenience. The other type of data was the elapsed time from the onset of the same green duration to the moment the rear bumper of the same vehicle crossed the stop line (for motion detection) or the downstream edge of the detector (for presence detection). This elapsed time will be defined as departure time. The arrival times and the departure times of the queueing vehicles were recorded simultaneously by two observers as audio signals on tape recorders. The signals were then decoded with a strip chart recorder.

In addition to the data specific to each queueing vehicle, the queueing position of the first vehicle upstream of a detector at the onset of a green duration was recorded for each observed queue. This information serves as a basis for correlating the arrival time of a vehicle with the departure time of another vehicle. The number of queueing vehicles ahead of the first queueing vehicle upstream of the detector varies from one queue to another. It can affect arrival times and, therefore, was included in the data collection.

QUEUE DISCHARGE HEADWAYS

The operations of both pulse control and presence control are influenced by the departure times of queueing vehicles after a green duration begins. The departure time, D_i, of a vehicle can be represented by the sum of a series of queue discharge headways:

$$D_i = \sum_{K=1}^{i} H_K \quad (1)$$

where H_K is the queue discharge headway of a vehicle in the Kth queueing position.

As given in Table 1 the average queue discharge headway (m) of the straight-through vehicles on Almond Street was 3.1 sec for vehicles in the first queueing position. This was based on a sample size (N) of 256 queues. The average headways fell to 2.5 sec for vehicles in the second queueing position and rapidly leveled off to about 2.1 sec. The standard deviations (S) of the queue discharge headways were in the range of 0.5 to 0.9 sec.

The left-turn vehicles on Erie Boulevard had average queue discharge headways 0.1 to 0.3 sec longer than the averages for the straight-through vehicles on Almond Street. However, the standard deviations of their discharge headways were also in the range of 0.5 to 0.9 sec. The average headways of the left-turn vehicles on Almond Street were up to 0.2 sec longer than those observed on Erie Boulevard. This is probably due to more restricted geometric design features (e.g., 8-ft lanes) encountered on Almond Street.

The cumulative distributions of the discharge headways of the vehicles in the first queueing positions were distinctly different from those of the others. Significant variations were also present among the distributions of the headways of those vehicles not in the first queueing positions. These variations were largely associated with headways of between 2 and 3 sec. The ranges of the observed headways decrease from about 6 seconds for vehicles in the first queueing position to about 4 seconds for those in the eight and ninth positions.

For each of the queueing positions given in Table 1, the cumulative distribution of the discharge headways can be replaced by a cumulative distribution of the discharge headways as percentage of the mean headway. This requires the headways, t, in the table to be converted into the percentages of the mean, m. With this simple manipulation, an interesting characteristic of the discharge headways emerges. As shown in Figure 2, the headway distributions for the various queueing positions can be realistically represented by a single normalized distribution for both straight-through and left-turn movements.

This normalized distribution can be used in several ways for simulating the discharge headways. Let

p = percentage of the mean headway for a given queueing position and
w = probability of a headway being less than or equal to p.

Then, one convenient way is to represent the distribution in terms of the following five linear equations:

$$p = 40 + 300\,w \quad \text{if } w \leq 0.1 \quad (2a)$$
$$p = 64 + 63\,w \quad \text{if } 0.1 < w \leq 0.5 \quad (2b)$$
$$p = 53 + 83\,w \quad \text{if } 0.5 < w \leq 0.8 \quad (2c)$$
$$p = 13 + 134\,w \quad \text{if } 0.8 < w \leq 0.95 \quad (2d)$$
$$p = -1{,}380 + 1{,}600\,w \quad \text{if } w > 0.95 \quad (2e)$$

In a simulation process w can be generated as a random number with a value between 0 and 1. The p value associated with this w can then be determined from one of the above equations. Multiplying this p by the mean headway for the corresponding queueing position results in a headway that belongs to the observed distribution.

TABLE 1 Cumulative Distribution of Queue Discharge Headways (H_K)

Headway t (sec)	Probability of $H_K \leq t$ Queueing Position 1	2	3	4	5	6	7	8	9
	a) Straight-Through Vehicles on Almond								
1.0	0.00	0.00	0.00	0.00	0.00	0.00	0.00	0.00	0.00
1.5	0.01	0.03	0.07	0.07	0.12	0.10	0.10	0.14	0.12
2.0	0.09	0.25	0.35	0.40	0.47	0.43	0.38	0.52	0.51
2.5	0.26	0.53	0.71	0.72	0.75	0.75	0.71	0.89	0.78
3.0	0.49	0.79	0.87	0.89	0.91	0.92	0.87	0.94	0.97
3.5	0.75	0.93	0.96	0.97	0.98	0.97	0.98	0.98	1.00
4.0	0.86	0.97	0.98	0.99	1.00	0.99	1.00	0.99	1.00
4.5	0.92	0.98	1.00	0.99	1.00	0.99	1.00	1.00	1.00
5.0	0.95	0.99	1.00	1.00	1.00	1.00	1.00	1.00	1.00
5.5	0.98	0.99	1.00	1.00	1.00	1.00	1.00	1.00	1.00
6.0	1.00	1.00	1.00	1.00	1.00	1.00	1.00	1.00	1.00
m	3.1	2.5	2.3	2.2	2.1	2.2	2.2	2.0	2.1
S	0.9	0.9	0.7	0.6	0.6	0.6	0.6	0.6	0.5
N	256	256	256	241	206	157	115	86	59
	b) Left-Turn Vehicles on Erie								
1.0	0.00	0.00	0.00	0.00	0.00	0.00	0.00	0.00	0.00
1.5	0.01	0.03	0.05	0.04	0.08	0.05	0.08	0.04	0.04
2.0	0.05	0.23	0.26	0.33	0.31	0.33	0.36	0.28	0.48
2.5	0.19	0.53	0.55	0.64	0.66	0.58	0.58	0.67	0.78
3.0	0.45	0.77	0.83	0.87	0.88	0.77	0.80	0.89	0.93
3.5	0.64	0.90	0.93	0.95	0.98	0.92	0.92	0.98	0.98
4.0	0.79	0.95	0.99	0.98	0.98	0.96	0.96	1.00	1.00
4.5	0.89	0.99	1.00	0.99	0.99	0.99	0.99	1.00	1.00
5.0	0.94	0.99	1.00	1.00	0.99	1.00	1.00	1.00	1.00
5.5	0.99	1.00	1.00	1.00	1.00	1.00	1.00	1.00	1.00
6.0	1.00	1.00	1.00	1.00	1.00	1.00	1.00	1.00	1.00
m	3.2	2.6	2.5	2.4	2.3	2.5	2.4	2.3	2.2
S	0.9	0.7	0.7	0.6	0.6	0.8	0.7	0.5	0.5
N	175	146	152	141	131	120	85	57	46

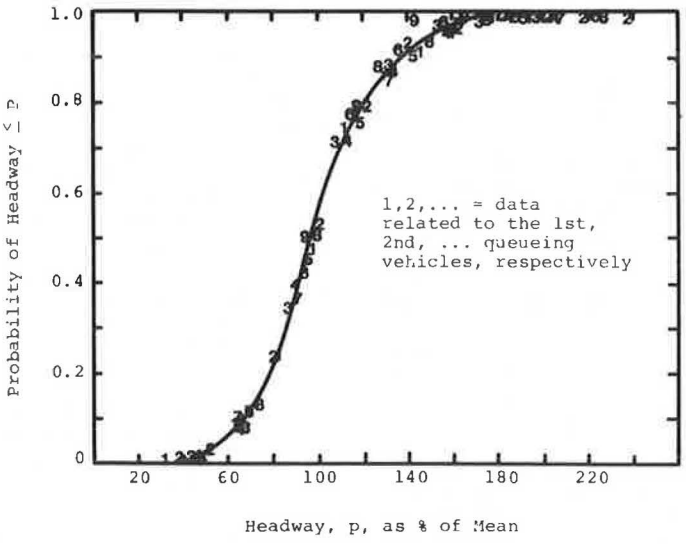

FIGURE 2 Normalized cumulative distribution of departure headways.

ARRIVAL CHARACTERISTICS

Let

f = queueing position of the first vehicle upstream of a detector at the onset of a green duration (Figure 1),
A_f = arrival time of the fth queueing vehicle, and
T_K = arrival headways of queueing vehicles behind the first upstream queueing vehicle (K = f + 1, f + 2, ...).

Then the arrival time, A_i, of a queueing vehicle in the ith queueing position can be determined as

$$A_i = A_f + \sum_{K=f+1}^{i} T_K \quad i > f \tag{3}$$

The value of A_f can be affected by the movement of the vehicle in the (f-1)th queueing position. This vehicle is the one just ahead of the first queueing vehicle upstream of a detector at the onset of a green duration. It is also the last queueing vehicle that has reached the detector by the time the green

light is turned on (Figure 1). Let the departure time of this leading vehicle be denoted as D_{f-1}. The field data show that the following general relationship exists between A_f and D_{f-1}:

$$A_f = V(D_{f-1}) \pm R \quad (4)$$

where $V(D_{f-1})$ is a deterministic component of A_f expressed as a function of D_{f-1} and R is a probabilistic component representing the variations of A_f from $V(D_{f-1})$.

A typical relationship between A_f and D_{f-1} is shown in Figure 3. Table 2 gives a summary of the specific forms of Equation 4 as determined from the field data. The variations of A_i from $V(D_{f-1})$ were found to be mostly less than 1.5 sec. This implies that the values of R range from 0 to 1.5 sec. Existing data, however, are not sufficient to determine the distribution of R at a given level of D_{f-1}.

The use of the equations in Table 2 requires the determination of D_{f-1} first. D_{f-1} depends very much on the position of the (f-1)th queueing vehicle. This position corresponds to the number of queueing vehicles that are at least partly inside the area defined by L (Figure 1) at the onset of a green duration. The data in Table 3 indicate that, for a given detector placement, this number cannot be reasonably assumed to be a constant. Therefore, a simulation analysis should also take this characteristic into consideration. Otherwise, systematic underestimates or overestimates of A_f will result.

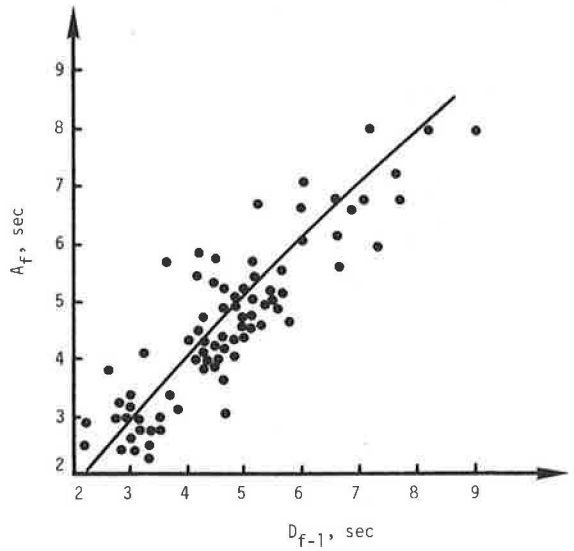

FIGURE 3 A_f - D_{f-1} relationship of straight-through queueing vehicles on Almond Street (L = 30 ft).

In contrast to A_f, the arrival headway T_K in Equation 3 can be conveniently determined from an observed distribution of arrival headways. The cumulative distributions of the arrival headways observed at the study sites are given in Tables 4 and 5. The means, standard deviations, and ranges of these distributions follow a pattern similar to those of the queue discharge headways.

Again, each of the distributions given in Tables 4 and 5 can be normalized by expressing the headways as percentages of the respective means. It can be shown that the resultant distributions are virtually the same as the one shown in Figure 2. Thus, the departure headways and the arrival headways may be governed by the same natural law regardless of the queueing position of a vehicle. If this is true, the input requirements for achieving a realistic simulation of the vehicle-detector interactions can be significantly reduced.

PREMATURE TERMINATION OF GREEN

Presence Control

Under a presence control a vehicle can demand right-of-way and hold the green by staying in a detection area. After a vehicle departs from the detection area, the green is continued for a period equal to a specified extension interval. If no detector actuations take place during this extension interval, the green could be terminated. This condition for holding the green can be represented by

$$D_{i-1} - \beta_{i-1} + E \geq A_i + \alpha_i \quad (5a)$$

or

$$A_i - D_{i-1} \leq E - \alpha_i - \beta_{i-1} \quad (5b)$$

where A_i and D_{i-1} are, respectively, the arrival time of the ith queueing vehicle and the departure time of the (i-1)th queueing vehicle; E is the ex-

TABLE 2 A_f - D_{f-1} Relationships

L(ft)	Equation
a) Straight-Through Flows on Almond	
30	$A_f = -0.900 + 1.450\ D_{f-1} - 0.050\ D_{f-1}^2 \pm R$
50	$A_f = -1.875 + 1.300\ D_{f-1} - 0.025\ D_{f-1}^2 \pm R$
80	$A_f = -1.615 + 1.029\ D_{f-1} - 0.018\ D_{f-1}^2 \pm R$
120	$A_f = 0.332 + 0.701\ D_{f-1} - 0.008\ D_{f-1}^2 \pm R$
b) Left-Turn Flows on Almond and Erie	
30	$A_f = -0.195 + 1.164\ D_{f-1} - 0.033\ D_{f-1}^2 \pm R$
50	$A_f = -1.525 + 1.050\ D_{f-1} - 0.017\ D_{f-1}^2 \pm R$
80	$A_f = -4.369 + 1.617\ D_{f-1} - 0.050\ D_{f-1}^2 \pm R$

TABLE 3 Percent of Queues with M Vehicles Fully or Partially in the Area Defined by L

M	Straight-Through on Almond L(ft)				Left Turns on Almond and Erie L(ft)			
	30	50	80	120	30	50	50[1/]	80
1	48.1	-	-	-	34.5	-	-	-
2	51.9	57.1	1.9	-	55.2	66.7	38.0	-
3	-	42.9	38.9	-	10.3	33.3	62.0	50.0
4	-	-	59.2	12.5	-	-	-	50.0
5	-	-	-	53.1	-	-	-	-
6	-	-	-	34.4	-	-	-	-

1/ On Almond Street

TABLE 4 Cumulative Distributions of Arrival Headways (T_K) of Straight-Through Vehicles on Almond Street.

Headway t (sec)	Probability of $T_K \leq t$ Position f+1	f+2	f+3	f+4	f+5	Position f+1	f+2	f+3	f+4	f+5
	a) L = 30 ft					b) L = 50 ft				
1.0	0.00	0.00	0.00	0.00	0.00	0.00	0.00	0.00	0.00	0.00
1.5	0.00	0.01	0.00	0.00	0.06	0.00	0.01	0.09	0.07	0.15
2.0	0.06	0.22	0.27	0.24	0.35	0.09	0.29	0.40	0.56	0.45
2.5	0.33	0.61	0.75	0.60	0.71	0.34	0.69	0.69	0.80	0.90
3.0	0.59	0.84	0.93	0.88	0.82	0.60	0.84	0.93	0.97	1.00
3.5	0.82	0.97	0.95	1.00	1.00	0.82	0.97	1.00	1.00	1.00
4.0	0.95	0.99	1.00	1.00	1.00	0.91	1.00	1.00	1.00	1.00
4.5	0.99	0.99	1.00	1.00	1.00	0.99	1.00	1.00	1.00	1.00
5.0	0.99	1.00	1.00	1.00	1.00	1.00	1.00	1.00	1.00	1.00
5.5	1.00	1.00	1.00	1.00	1.00	1.00	1.00	1.00	1.00	1.00
m	2.9	2.4	2.3	2.5	2.1	2.9	2.3	2.2	2.1	2.0
S	0.6	0.5	0.5	0.5	0.5	0.8	0.6	0.5	0.5	0.4
N	84	66	44	25	17	95	68	45	30	20
	c) L = 80 ft					d) L = 120 ft				
1.0	0.00	0.00	0.00	0.00	0.00	0.00	0.00	0.00	0.00	0.00
1.5	0.00	0.02	0.07	0.16	0.07	0.00	0.00	0.08	0.10	0.00
2.0	0.10	0.25	0.36	0.42	0.53	0.03	0.09	0.33	0.19	0.22
2.5	0.23	0.58	0.64	0.74	0.67	0.17	0.59	0.69	0.51	0.67
3.0	0.48	0.88	0.89	0.95	0.93	0.59	0.83	0.92	1.00	0.94
3.5	0.65	0.98	0.96	1.00	1.00	0.79	0.96	0.92	1.00	1.00
4.0	0.83	0.98	1.00	1.00	1.00	0.93	1.00	0.96	1.00	1.00
4.5	0.92	0.98	1.00	1.00	1.00	0.93	1.00	1.00	1.00	1.00
5.0	0.98	0.98	1.00	1.00	1.00	0.97	1.00	1.00	1.00	1.00
5.5	1.00	1.00	1.00	1.00	1.00	1.00	1.00	1.00	1.00	1.00
m	3.2	2.5	2.3	2.1	2.2	3.1	2.4	2.3	2.4	2.4
S	0.9	0.7	0.6	0.6	0.5	0.7	0.4	0.8	0.5	0.4
N	48	40	28	19	15	29	27	26	21	18

tension interval; β_{i-1} represents the departure response time (i.e., the time required for a detector to recognize the departure of a vehicle before the rear bumper of the vehicle crosses the downstream edge of a detector); and α_i is the arrival response time (i.e., the time required for a detector to recognize the arrival of a vehicle after the front bumper of the vehicle crosses the upstream edge of the detector).

The arrival response time, α_i, and the departure response time, β_i, of a loop presence detector depend in part on the sensitivity of the detector and the type of vehicle. They are also a function of individual vehicle speed. In a field test using a 1981 Reliant K over a 62-ft-long detector, it was found that the front bumper has to be 2.5 to 3 ft inside the detector to actuate the detector. The same test also showed that the rear bumper should be at least about 2 ft inside the downstream end of the detector to hold the green. Therefore, a vehicle traveling at a constant speed of 10 mph would have an α_i of just under 0.2 sec and a β_i of approximately 0.13 sec. For a given detector length, queueing vehicles further upstream from the detector would have lower α_i and β_i than those closer to it because of their higher speeds.

The right-hand side of Equation 5b can be referred to as adjusted extension interval. To prevent premature termination of a green duration, the value of A_i minus D_{i-1} cannot exceed the corresponding adjusted extension interval. For a given adjusted extension interval, the chance of premature termination of a green duration increases as the length of the detection area is shortened. This characteristic is shown in Figure 4 in terms of the observed rela-

TABLE 5 Cumulative Distributions of Arrival Headways (T_K) of Left-Turn Vehicles on Almond and Erie streets.

Headway t (sec)	Probability of $T_K \leq t$ Position f+1	f+2	f+3	f+4	f+5	Position f+1	f+2	f+3	f+4	f+5
	a) L = 30 ft (Erie)					b) L = 50 ft (Erie)				
1.0	0.00	0.00	0.00	0.00	0.00	0.00	0.00	0.00	-	-
1.5	0.00	0.04	0.07	0.08	0.07	0.00	0.05	0.00	-	-
2.0	0.14	0.46	0.35	0.58	0.40	0.09	0.17	0.33	-	-
2.5	0.41	0.88	0.57	0.89	0.87	0.26	0.62	0.80	-	-
3.0	0.79	0.96	0.83	0.89	0.93	0.59	0.90	0.87	-	-
3.5	0.93	0.96	1.00	1.00	0.93	0.85	1.00	1.00	-	-
4.0	0.93	1.00	1.00	1.00	1.00	0.85	1.00	1.00	-	-
4.5	1.00	1.00	1.00	1.00	1.00	0.96	1.00	1.00	-	-
5.0	1.00	1.00	1.00	1.00	1.00	1.00	1.00	1.00	-	-
m	2.7	2.1	2.4	2.0	2.3	2.9	2.4	2.3	-	-
S	0.6	0.5	0.6	0.5	0.8	0.7	0.5	0.5	-	-
N	29	24	23	19	15	27	21	15	-	-
	c) L = 80 ft (Erie)					d) L = 50 ft (Almond)				
1.0	0.00	0.00	0.00	0.00	-	0.00	0.00	0.00	0.00	0.00
1.5	0.00	0.04	0.04	0.17	-	0.00	0.00	0.03	0.00	0.04
2.0	0.12	0.46	0.36	0.52	-	0.06	0.12	0.21	0.21	0.22
2.5	0.33	0.75	0.75	0.78	-	0.23	0.47	0.67	0.59	0.63
3.0	0.64	0.89	0.93	0.96	-	0.57	0.81	0.92	0.82	0.89
3.5	0.85	0.96	0.96	0.96	-	0.87	0.95	1.00	0.94	1.00
4.0	1.00	1.00	1.00	1.00	-	0.89	1.00	1.00	1.00	1.00
4.5	1.00	1.00	1.00	1.00		0.94	1.00	1.00	1.00	1.00
5.0	1.00	1.00	1.00	1.00		0.96	1.00	1.00	1.00	1.00
5.5	1.00	1.00	1.00	1.00		1.00	1.00	1.00	1.00	1.00
m	2.9	2.2	2.3	2.2		3.0	2.6	2.4	2.5	2.4
S	0.6	0.6	0.6	0.7		0.8	0.5	0.4	0.6	0.5
N	33	28	28	23		47	43	39	33	27

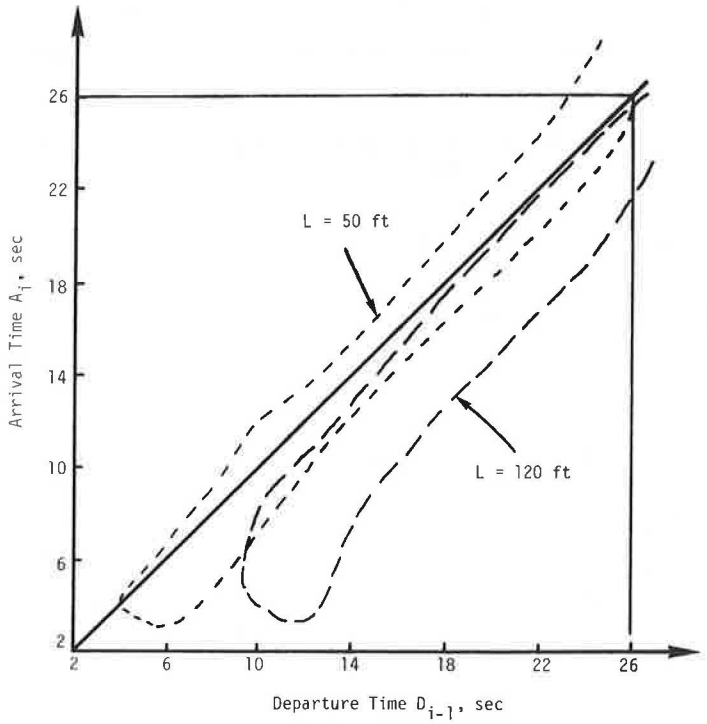

FIGURE 4 Domains of observed correlations between A_i and D_{i-1} of straight-through queueing vehicles on Almond Street.

tionship between A_i and D_{i-1} for the straight-through queueing vehicles on Almond Street. With a 120-ft detector, D_{i-1} exceeded A_i in all the observations. This implies that a 120-ft detector allows a queueing vehicle to actuate the detector before the vehicle ahead leaves the detection area. Consequently, premature termination of a green duration is an unlikely event. In contrast, a large number of the observed queueing vehicles had $A_i > D_{i-1}$ for a detector 50 ft long. In such a

case, a short adjusted extension interval can lead to frequent premature termination of green durations.

Figure 5 shows the probabilities of premature termination of a green duration for detector lengths of 30 and 50 ft. These probabilities were determined from the field data by considering only one traffic lane. The corresponding probabilities for detector lengths greater than 80 ft are not shown because they are negligibly small. It is evident from Figure 5 that the use of detectors shorter than 50 ft will require a careful selection of an extension interval to avoid premature termination of a green duration.

The probabilities shown in Figure 5 can be reduced if more than one lane is associated with a signal phase. To what extent the probabilities can be reduced, however, depends on the actual traffic and signal control conditions.

Premature termination of a green duration is usually undesirable. To prevent it or to lessen the chance of its occurring, long detectors can be used. This alternative, however, would increase the dwell time of a vehicle in a detection area (Figure 6). The dwell time is the time a vehicle spends in a detection area after a green duration begins. A long dwell time of a vehicle results in sluggish transfers of right-of-way and, thus, may increase delays. Another alternative to ease the problem is to use short detectors in conjunction with long extension intervals. It is still not clear, however, what combinations of detector length and extension interval would result in high control efficiencies.

Motion Control

When a motion control is employed, premature termination of a green duration is governed primarily by the formation of queues and by the settings of initial interval and vehicle interval. Following actuation by a vehicle, a motion detector requires a short time to produce a pulse. This time interval varies with the make and the sensitivity setting of the detector and ranges from about 4 milliseconds to about 200 milliseconds. The pulse duration is usually 75 to 150 milliseconds per vehicle unless a vehicle stalls in the detection area. The time required for a detector to sense the arrival of a vehicle is also very short. Moving a 1973 Valiant over a detector 6 ft long, it was found that the detector can be actuated when the front bumper is less than 1.5 ft inside the detector. This is equivalent to an arrival response time of about 0.1 sec at a vehicle speed of 10 mph.

The elapsed time between two successive actuations of a detector is $A_{i+1} + \beta_{i+1} - A_i - \beta_i$ or $T_{i+1} + \beta_{i+1} - \beta_i$. This elapsed time should be shorter than the vehicle interval in order to extend a green duration. The difference between $\beta_{i+1} - \beta_i$ is likely very small. Therefore, the headway T_{i+1} should be shorter than the vehicle interval in order to extend a green duration.

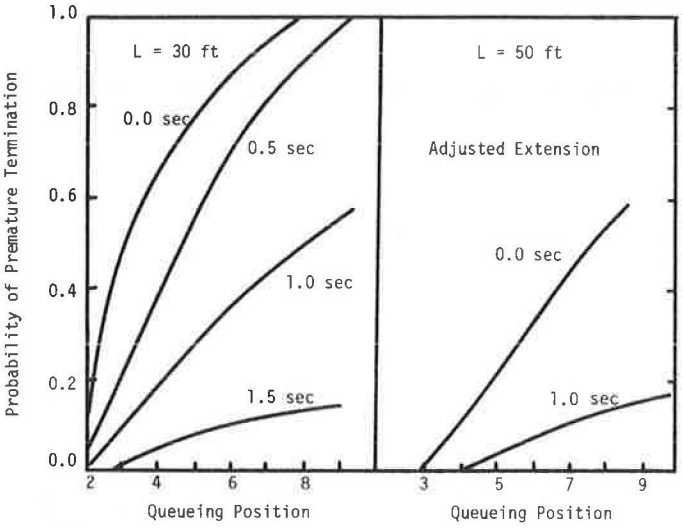

FIGURE 5 Probabilities of premature termination of green under a presence control (single lane flow).

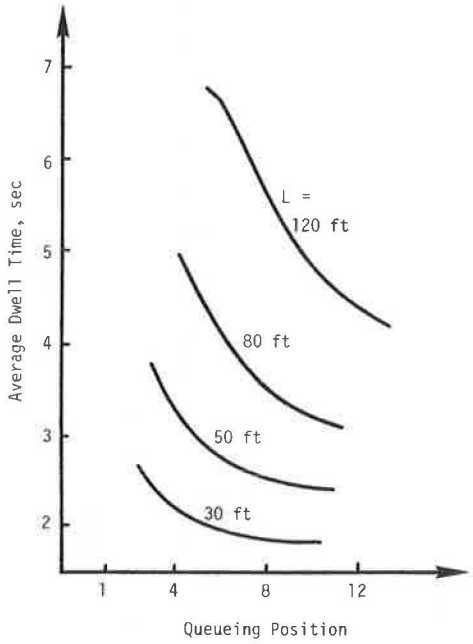

FIGURE 6 Average dwell time as a function of L and queueing position.

It can be seen from Tables 4 and 5 that arrival headways of less than 1.0 sec did not exist at the study sites. Furthermore, the probability of an arriving headway being less than 2 sec was very low for the queueing vehicles just upstream of a detector. Therefore, if a queue extends upstream of a detector, the use of a vehicle interval of 2 sec can easily result in premature termination of a green duration. This can be illustrated with a simple example.

Consider a motion control with a detector setback of 80 ft. At the beginning of a green duration there are six queueing vehicles upstream of the detector. Assume that the first three vehicles (f, f+1, and F+2) can either cross the detector during the initial interval or extend the green duration. The vehicle interval is set at 2 sec. The problem is to determine the probability of premature termination of the green for the remaining three vehicles.

Based on the data in Table 4 for L = 80 ft, the approximate probabilities that vehicles f+3, f+4, and f+5 will extend a green duration are, respectively, 0.36, 0.42, and 0.53. Therefore, the probability that at least one of these three vehicles will be unable to extend the green duration is 1 - 0.36 x 0.42 x 0.53 = 0.92. Even with a vehicle interval of 2.5 sec, the corresponding probability of premature termination of the green duration is still 0.73. For this reason, it is unlikely that vehicle intervals as short as 1 or 2 sec can improve the performance of a motion control under a wide range of traffic flow conditions.

IMPLICATIONS

The vehicle-detector interactions described previously could create several problems in the analysis of a control. One major problem is the danger of generating misleading information when such interactions are not properly accounted for. This danger is illustrated with two examples shown in Figure 7 for a full-actuated motion control and in Figure 8 for a presence control. In both examples a two-phase operation with two lanes in each phase was examined through computer simulation. The analysis relied on

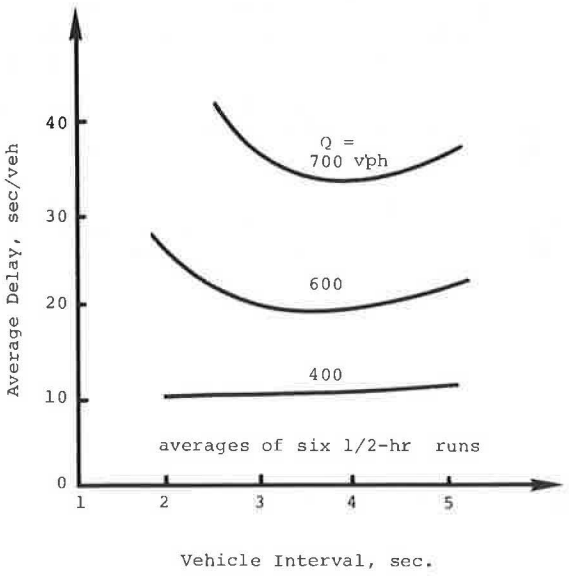

FIGURE 7 Average vehicle delay as a function of vehicle interval and flow rate for L = 120 ft (pulse control).

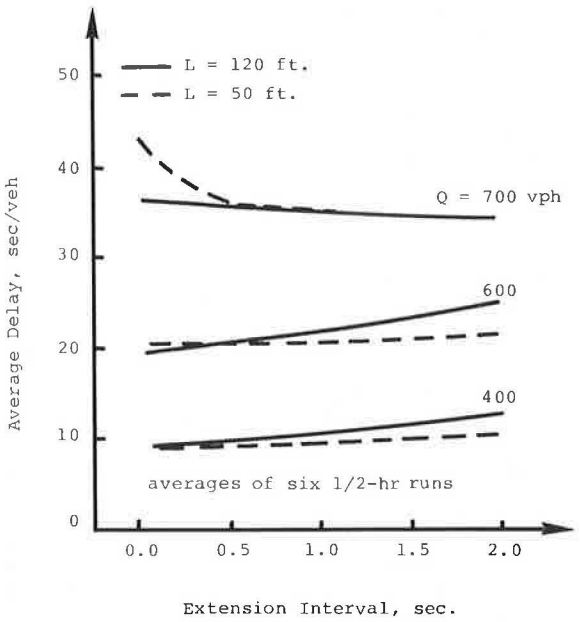

FIGURE 8 Average delay as a function of detector length, extension interval, and flow rate (presence control).

a simulation model (RAPID) that was developed at Clarkson College of Technology. In the analysis, the traffic volume, Q, was assumed to be the same in all lanes. Only straight-through vehicles were considered. And the observed vehicle-detector interactions shown in Tables 1-4 for such vehicles were used as input in the simulation.

For the motion control, the initial interval, maximum green, and clearance interval were, respectively, 10, 50, and 4 sec for either phase. The initial interval was followed automatically by one vehicle interval. The detector setback was 120 ft. And the same maximum green and clearance intervals were used for the presence control.

Contrary to the findings of other studies, Figure 7 shows that, for a motion control, shortening the vehicle interval will not necessarily reduce the delays. When traffic flows are light (e.g., Q = 400 vph/lane), the chance for queues to extend beyond a detector with 120 ft in setback is slim. Under this condition premature termination of a green duration is unlikely to occur. As a result, the average delays become insensitive to the vehicle interval. With heavier flows long queues may exist in most of the cycles. Consequently, the use of short vehicle intervals makes it difficult for many queueing vehicles to extend green durations to satisfy their needs. This explains why in Figure 7 vehicle intervals of less than 3 sec increase delays substantially for flows of 600 and 700 vph/lane.

Similarly, Figure 8 shows that, under a presence control, a short detector length (L = 50 ft) is not always better than a long one (L = 120 ft). This is a characteristic not identified in other studies. The use of 120-ft-long detectors virtually eliminates premature termination of a green duration, but it produces long dwell times. As expected, delays increase with the extension interval under light flow conditions. When 50-ft-long detectors are used, the interplays between premature termination, dwell time, and extension interval could give rise to inefficient controls. For example, an extension interval of 0.0 sec allows the operation of a control to be dominated by premature termination of a green duration. This, in turn, brings about excessive delays under heavy flow conditions.

Obviously misleading or unrealistic simulation results would only raise doubts in the minds of informed engineers about the reliability of a simulation model. More serious consequences may emerge if such results are accepted by unwary users. Errors in simulation results caused by improper modeling of flow characteristics are usually difficult to detect. Therefore, it is advisable that simulation models be calibrated with observed vehicle-detector interactions.

Another problem in dealing with the vehicle-detector interactions is related to the sensitivity of signal operations to such interactions. A high sensitivity would require accurate input data or demand more simulation runs. A low sensitivity could tolerate greater errors in the measurement of the interactions. Of particular concern in this regard are the A_f-D_{f-1} relationship, the values of the detector response times α_i and β_i, and the distributions of the queue discharge headways and the arrival headways.

The measured relationship between A_f and D_{f-1} may be biased by the discrepancies in observers' reactions to the beginning of a green duration. The experience gained in this study indicates that the discrepancies can be confined to a value of less than 0.3 sec. Allowing the value of A_f to increase or decrease by 0.3 sec from those estimated from the equations given in Table 3, the resultant simulated average delays differ by less than 0.4 sec per vehicle. For all practical purposes, such differences are not significant. Varitions in α_i and β_i of up to 0.3 sec are also found to have negligible impact on control efficiency.

On the other hand, variations in the queue discharge headways and the arrival headways could have significant effects. For example, let the distributions of the straight-through headways given in Tables 1 and 4 be shifted by 0.15 sec to shorter headways. This shift results in substantial reductions in the average delays presented in Figures 7 and 8 for Q = 600 and 700 vph/lane. The reductions reach as high as 20 to 30 percent, particularly when the problem of premature termination of a green duration exists. Therefore, the accurate representation of the distributions of queue discharge headways and arrival headways is of foremost concern in the analysis of a traffic-actuated control.

CONCLUSIONS

The vehicle-detector interactions under a traffic-actuated control can be characterized by (a) queue discharge headway, (b) arrival headway, (c) the A_f-D_{f-1} relationship, (d) the number of queueing vehicles in the area defined by L (Figure 1) at the onset of a green duration, and (e) dwell time. These flow characteristics are probabilistic entities and should be treated as such. For simulation analysis of a traffic-actuated control, a model should be calibrated in terms of the observed characteristics of such parameters and relationships.

For both straight-through and left-turn queueing vehicles, the distributions of the observed queue discharge headways and arrival headways were found to follow similar trends. When the headways are expressed as percentages of the means for respective queueing positions, these distributions can be replaced by a single normalized distribution.

The difficulty observers have starting measurement simultaneously in response to the beginning of a green duration can bias the observed A_f-D_{f-1} relationships. The biases, however, are small and do not significantly affect simulated vehicle delays. The arrival response time and the departure response time of a detector are not fully understood. Nevertheless, they appear to be rather short, corresponding to the time required for a vehicle to travel a distance of 2 to 3 ft. Their effects on vehicle delays also seem to be negligible. In contrast, vehicle delays are rather sensitive to the distribution of queue discharge headways.

Under a presence control, the chance for premature termination of a green duration increases when detector lengths are shortened. A detector length of longer than 80 ft can effectively eliminate the premature termination. Using long detectors, however, results in long dwell times and may thus reduce control efficiency. The tradeoffs between long detectors and short detectors are not well understood at present.

Arrival headways of less than 2 sec constitute only a small portion of the observed headways. Therefore, when a vehicle interval of 1 or 2 sec is used, a motion control cannot be expected to achieve a high control efficiency under a wide range of traffic conditions. A simulation model should be capable of revealing such a characteristic.

This study demonstrates the need to assess existing simulation models that are being used for the analysis of traffic-actuated control. Before a model is used and a conclusion drawn, one should make sure that the model has an adequate representation of the vehicle-detector interactions. Otherwise, misleading information may be generated.

REFERENCES

1. R.W.T. Morris and P.G. Pak-poy. Intersection Control by Vehicle-Actuated Signals. Traffic Engineering and Control, Oct. 1967, pp. 288-293.
2. P.G. Michalopoulos, B. Papapanou, and E.B. Binseel. Performance Evaluation of Traffic Actuated Signals. Journal of the Transportation Engineering Division of ASCE, Vol. 104, No. TE5, Sept. 1978, pp. 621-636.
3. R.D. Worral and E. Lieberman. Network Flow Simulation for Urban Traffic Control Systems, Vol. 1-5. FHWA, U.S. Department of Transportation, 1973.
4. Traffic Network Analyses with NETSIM-A User Guide. Implementation Package FHWA-IP-80-3. FHWA, U.S. Department of Transportation, Jan. 1980.
5. P.J. Tarnoff and P.S. Parsonson. Selecting Traffic Signal Control at Individual Intersections. NCHRP Report 233. TRB, National Research Council, Washington, D.C., June 1981, 133 pp.

Publication of this paper sponsored by Committee on Traffic Flow Theory and Characteristics.

could be gained under controlled conditions on a scale that generally precludes real-world experimentation.

In addition, the simulations will address a proposed extension (1) of the two-fluid model that postulates a relation between the fraction of time stopped, f_s, and the network concentration, K, of the form

$$f_s = (K/_m)^p \quad (3)$$

where K_m is the average maximum concentration level at which the network jams (in a sense, a network-level parallel to the jam concentration of an arterial) and p is a network-specific parameter reflecting the sensitivity of f_s to increasing levels of use. Combining their expression with the previous equations of the two-fluid model yields (1)

$$K = K_m[1-(V/V_m)^{(1/n+1)}]^{1/p} \quad (4)$$

The relationship between K and V ties the two-fluid concept to the earlier discussion of a network traffic flow theory.

Flow Distribution on Network Components

In addition to the network performance models discussed previously, the distribution of traffic on various components of the network will be examined. The importance of this question is primarily methodological in that it relates to the design of simulation experiments to examine the circulation of vehicles in a network under controlled conditions.

As will be seen in the next section, an attempt has been made to maintain a certain degree of homogeneity and uniformity within each experiment (at least in these early stages) to avoid unnecessary complications that would make insights more difficult to obtain. A question arises about whether there are long-term trends of traffic distributing itself in some parts of the network to the exclusion of others. For instance, for a given (closed) test network configuration and control system and a given set of parameters governing the movement of vehicles on that network (i.e., the inputs to the simulation model), particular circulatory patterns involving only those links that define the boundary of the study network might be observed. This issue will become clearer in the next section in the context of the description of the test network and of the other details of the simulation experiments.

EXPERIMENTAL DESIGN AND SETUP

In all simulations, interest was in the network-level properties of a fixed number of vehicles circulating in a closed system. Thereby a constant concentration of vehicles in the network throughout the simulation period was maintained. Although the same network configuration was used in all the experiments, the traffic characteristics (including usage patterns) as well as the control strategy were varied. Two groups of simulation runs were performed, each group corresponding to a different combination of traffic characteristics and control strategy. Within each of the two groups, two parameters were varied across runs: (a) the concentration level (ranging from 1 to 75 vehicles per lane-mile) and (b) the mean "desired" speed, specified as either 25 or 35 mph (the desired speed of a given driver is the speed at which he would travel in the absence of other vehicles and traffic controls) (9).

Further details on these elements of the simulation experiments are presented hereafter, following a brief overview of the NETSIM model, which, as was noted earlier, was used to perform all of these experiments.

The NETSIM Model

NETSIM is a fixed-step, microscopic, network traffic simulation model, which was developed primarily as a tool for the analysis of alternative urban street network control and traffic management strategies. It is generally accepted as a well-validated model and has been used extensively by traffic researchers and engineers.

Each vehicle in the system is treated separately during the simulation. Vehicle behavior is governed by a set of microscopic car-following, queue-discharge and lane-switching rules. An array of performance characteristics is stochastically assigned to each vehicle as it enters the network. All vehicles are processed once every second and their time-space trajectory recorded to a resolution of 0.1 sec. [Further details are given elsewhere (9,10).] The NETSIM model was selected primarily for its high level of detail in the representation of microscopic traffic phenomena, its sensitivity to the factors of interest in the investigation, and its rather well-developed user-related features such as types of output and summaries.

Network Configuration and Geometric Features

As noted in the previous section, a degree of regularity and uniformity in the test network used at this stage of the investigation was sought. This network consists of 25 nodes, arranged in a 5 node by 5 node square, connected by two-way, four-lane streets forming a regular, central business district-like grid. Because only directed links should be used in representing the network in NETSIM (i.e., all links are one-way), there are 80 one-way, two-lane links, as shown in Figure 1. Each link (block) is 400 ft long, with no right- or left-turn bays, and all grades are zero.

Vehicles are injected onto the network via 12 entry links placed around the perimeter, three to a side, with each entry link connecting a source node (source nodes are labeled 801 to 812 in Figure 1) to

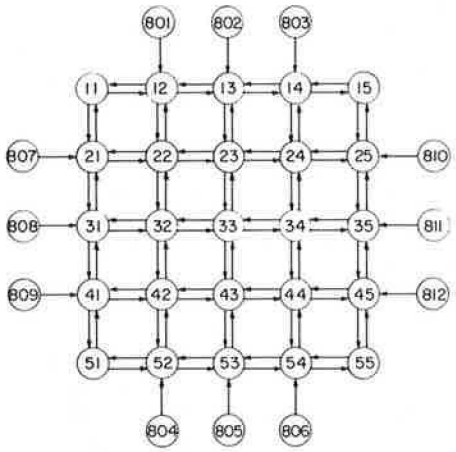

FIGURE 1 Network configuration (nodes 801-812 are source nodes and not part of the circulation network).

a noncorner boundary node. No sink nodes have been designated, because a closed system where vehicles remain in the network once they have entered it is under consideration.

Traffic Characteristics and Control Strategies

As mentioned previously, the simulations reported here belong to one of two groups. In the first group, vehicle turning movements were uniform throughout; at the interior nodes, one-third of all incoming vehicles (on any of the approaches incident to a given node) turned left, one-third turned right, and one-third continued straight through. At the boundary nodes, incoming traffic split equally between the two available options. Fixed-time traffic signals were placed at all 25 nodes, each with a 50-sec cycle length and a 50/50 split (i.e., green time equally divided between the intersecting streets), with no protected turning movements. All 25 signals were operated simultaneously, so that all the north and south approaches were green together, followed by all the east and west approaches.

In the second group, vehicle movements at the interior nodes were changed to 10 percent left, 15 percent right, and 75 percent through; they were not changed (relative to group 1) at the boundary nodes. A phase was added to the signals along the boundary to provide a protected left turn for vehicles reentering the interior of the system. The 50-sec cycle length was apportioned equally among the three approaches (phases); however, splits at the interior intersections were not changed. The four signals at the corner nodes were removed, thus allowing traffic to move unhindered through the corner nodes. Signals were operated according to a single alternative system whereby offsets between adjacent signals were all 50 percent of the cycle length so that, at any given time, every other signal along a street was green and the intervening signals were red.

There were no pedestrians, and right-turn-on-red was allowed at all intersections in both groups. Additional details of individual runs are presented next.

Individual Runs

A 5-min start-up period was used in all runs during which vehicles were generated uniformly on the 12 entry links. The vehicles were injected directly into the network interior by not allowing turns onto the boundary from the entry links. The vehicles were then allowed to circulate in the network for the desired simulation period (15 min for most of cases, although longer runs were made). Intermediate output was printed every minute, providing a "snapshot" of each link's condition at that time along with some cumulative information for each link. Network-level cumulative information as well as additional cumulative link data were printed every 3 min during the simulation period.

As mentioned earlier, two quantities were allowed to vary within each of the two groups. The mean desired speed in the network had an assumed value of either 25 or 35 mph in a given simulation. Vehicle concentration, which is a key quantity in these experiments, varied across a wide range of up to 75 vehicles per lane-mile. The results of these simulations are analyzed and critically discussed in the next section.

ANALYSIS OF SIMULATION RESULTS

The results of the simulation experiments conducted to date are analyzed with respect to those aspects of network traffic behavior identified earlier. The discussion is organized in the same three categories that were used in the conceptual background description, namely, flow distribution on network components, network traffic flow theory, and the two-fluid theory of town traffic.

Flow Distribution on Network Components

This aspect is discussed first because of its implications for the remainder of the analysis. In particular, the determination of the appropriate observation period, over which time averages of the network variables of interest were defined, was predicated on the results of the analysis of the long-run circulatory patterns developing in the test network. Two phenomena are investigated: the relative distribution of actual flow in the boundary links versus the interior links and the respective fractions of vehicles on boundary links and on interior links. In both cases, the chief concern is with the time-varying patterns of the quantities under consideration. Note that boundary links are defined as those one-way links, shown in Figure 1, with both end nodes belonging to the set of nodes {11, 12, 13, 14, 15, 21, 25, 31, 35, 41, 45, 51, 52, 53, 54, 55}. All other links, with the exception of the entry links, in the circulation network of Figure 1 are interior links.

To observe the dynamic behavior of the traffic measures pertaining to the relevant questions, a number of runs were conducted, each with 30 min of simulation beyond the initial 5 min required to load the network. The relative distribution of flow in boundary versus interior links is addressed first. Link flow can be calculated from the cumulative discharges given for each link in each intermediate output of the NETSIM model. The arithmetic averages of these minute-by-minute flows were taken separately over the boundary and interior links. These minute-by-minute boundary-average and interior-average flows are shown in Figure 2 for a representative simulation run. This run is from group 1 (groups 1 and 2 are used hereafter to denote the two combinations of traffic characteristics and control strategies described earlier).

As expected, average flows for both boundary and interior links start by increasing monotonically during and shortly after the network loading period. Subsequently, fluctuations can be observed, and there is a clear tendency for these fluctuations to occur around an apparently stable average value. The

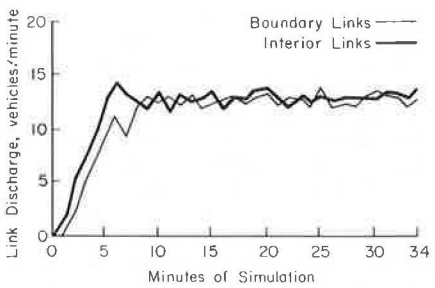

FIGURE 2 Link discharge for interior and boundary links.

system is considered stable when the link flows stabilize about an average value particular to each simulation. It can be seen in Figure 2 that this condition is achieved after approximately 8 min of total simulation time (i.e., 3 min after all the vehicles have been emitted at the source nodes). Furthermore, Figure 2 shows that the average flows for the boundary and interior links, respectively, have approximately the same value. The same conclusions could be reached for the other runs as well. Accordingly, it was decided to start the observation period, for the purpose of these analyses, at the 8th minute in all cases. In most runs analyzed, the observation period was ended at the 20th minute.

The second perspective from which to examine the general stability of the network is based on the respective fractions of vehicles on the boundary links and the interior links. In all cases, vehicles were injected directly into the interior of the network. Thereafter, given the rules governing turning movements at the intersections, vehicles eventually reached the boundary links, and, after some period of time, the fractions of vehicles on the boundary and interior links, respectively, seemed to stabilize about some constant value that was different for each of the two link classes. As is the case with average link flows, the network appears to be generally stable after about 8 min.

The time variation of the respective fractions of vehicles on the boundary and interior links for a representative 35-min run (also from group 1) are shown in Figure 3. These fractions were calculated on a minute-by-minute basis from tallies of link occupancies (separately for boundary and interior links) from the intermediate output of NETSIM. Figure 3 shows that, although the vehicle fractions undergo fluctuations, these appear to stabilize about a mean value of approximately 0.440 for boundary links and 0.560 for interior links for the simulation run under consideration. These values are actually extremely close to the arithmetic averages taken over all group 1 simulations. In this network, boundary links comprise 40 percent of the total network length, and the interior links comprise the remaining 60 percent. As the fractions here indicate, the boundary links have a higher average vehicle concentration than do the interior links. The results from the other group 1 runs are given in Table 1.

Vehicle fractions on the boundary and interior links for a simulation from group 2 are shown in Figure 4. Similar results were found for the other runs in group 2 and are given in Table 2. As in the previous cases, the network appears to stabilize after about 8 min of simulation, but the vehicle fractions on the links are different: 0.402 on the boundary links and 0.598 on the interior links. This is much closer to the ratio of total length of the boundary and interior links than is evident in the group 1 runs. The specified turning movements between groups 1 and 2 changed only for the interior intersections, and the primary cause of this change is probably the modified traffic signal phasing at the boundary nodes. The addition of a protected left-turn phase to allow traffic to more readily re-enter the network interior has apparently led to a reduction in vehicle concentrations on the boundary.

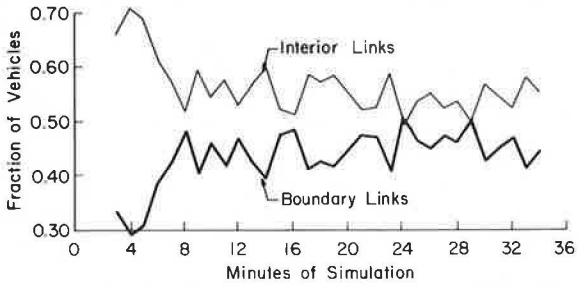

FIGURE 3 Fraction of vehicles on boundary and interior links, group 1.

TABLE 1 Average Fractions of Vehicles on Boundary and Interior Links (f_b and f_i), Group 1

	f_b	f_i
	0.440	0.560
	0.453	0.547
	0.460	0.540
	0.426	0.574
	0.424	0.576
Overall average	0.441	0.559

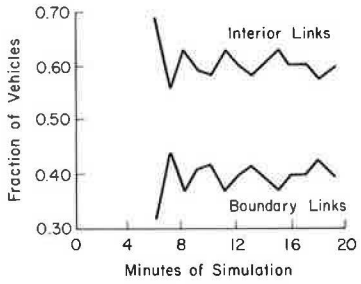

FIGURE 4 Fraction of vehicles on boundary and interior links, group 2.

TABLE 2 Average Fractions of Vehicles on Boundary and Interior Links (f_b and f_i), Group 2

	f_b	f_i
	0.395	0.605
	0.396	0.604
	0.394	0.606
	0.391	0.609
	0.400	0.600
	0.401	0.599
	0.416	0.584
	0.407	0.593
	0.398	0.602
	0.405	0.595
	0.425	0.575
	0.389	0.611
Overall average	0.402	0.598

Network Traffic Flow Theory

As discussed previously, the relationship between network concentration, K, and average speed, V, (both taken over the same observation period) is of prime interest. This was explored by varying concentration levels, K, while keeping all other features of the network, including the control system and the traffic characteristics, constant. For each

run, the average speed was found by dividing the total amount of time spent in the system by the vehicle-miles traveled. Both quantities were aggregated over the population of vehicles in the network between the 8th and 20th minutes of simulation, which defines the observation period for the reasons explained earlier in this section.

The average speeds thus obtained for a number of group 2 simulation runs (with a 35-mph mean desired speed) at different concentration levels of up to 75 vehicles per lane-mile are shown in Figure 5. Note

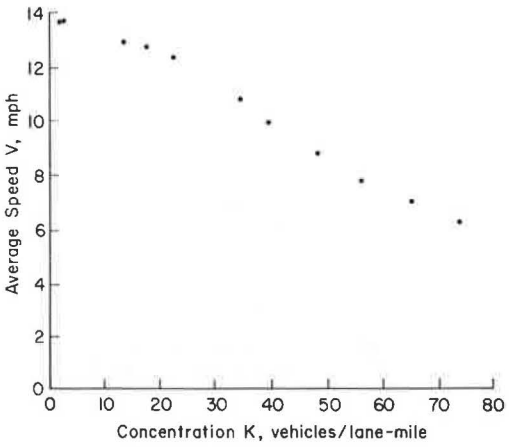

FIGURE 5 Average speed versus network concentration, group 2 runs (35 mph mean desired speed).

here that each point corresponds to an individual simulation run at a given concentration level and not to an average over a number of replicated runs [i.e., using different seeds for the random number generator underlying the stochastic features of NETSIM (9,10)] at the same concentration. Replications were not needed for the exploratory study because of the very large number of vehicles and the long observation periods over which the average quantities of interest were calculated. This was confirmed by a number of replications that were performed using different seeds for a variety of conditions, all of which yielded practically identical results for the averages under investigation (greater sensitivity to this aspect could, however, be problematic at very low concentration levels where stochastic effects are more pronounced). It can be seen in Figure 5 that the average network speed clearly decreases as a function of increasing network concentration. This is not unlike the K-V relationship that prevails on arterials. Particular care must be exercised in interpreting the extreme values (low K and high K); at the lower end of the concentration spectrum, the aforementioned stochastic effects might be prevalent, whereas at the higher end instabilities, which may not be adequately captured in the simulation, might arise. The results shown are nevertheless insightful because they reveal a clear qualitative trend between K and V. Note also that the rate of decrease of V slowly decreases at the higher concentration values shown in Figure 5.

To highlight the effect of the operational control system and associated traffic characteristics on the relationship between V and K, Figure 6 shows the average speeds obtained for a wider selection of simulation conditions under varying concentration

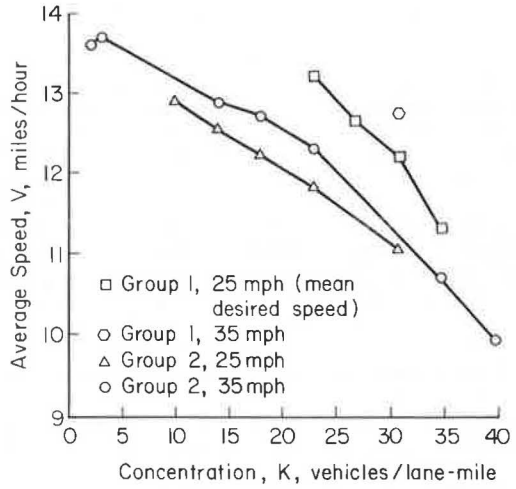

FIGURE 6 Comparison of average speed-network concentration relationship for various simulation groups.

levels but over a more restricted range. Thus both groups 1 and 2 are represented in Figure 6 at both mean desired speeds (25 and 35 mph). For each desired speed within each group, a separate K-V trend can be distinguished over the range of speeds and concentrations under consideration. Although there is only one reading for a group 1 simulation at 35-mph mean desired speed, it is included in Figure 6 because it clearly lies off the other three lines. It is apparent in Figure 6 that, within a given group, simulations conducted with a 35-mph mean desired speed displayed a higher average speed, for the same concentration level, than a corresponding run with 25-mph mean desired speed. Furthermore, the group 1 combination of traffic controls and operating characteristics resulted in better performance, in terms of average speed at a given concentration level, than did the group 2 combination at both mean desired speed levels. The main conclusion is that although average speed in a network shows a clear decreasing trend as network concentration increases, the trend itself seems to vary as a function of the operational characteristics and controls governing the use of the network configuration. However, considerable further probing is required before more generalizable conclusions can be reached.

Next the Q = KV relationship, discussed earlier, is investigated. The concentration, K, remains constant over the observation period during each simulation, and the speed is calculated as described previously. The average link flow, also defined earlier and used in determining network stability, is averaged over all links over the period between the 8th to 20th minutes of simulation. Because the link discharges represent the flow in each link and each link is identical (400 ft long, two-lane, and one-way), the average of the link discharges over the period of time in question represents the average flow seen by an average point of the network. The results for a selected number of simulations (corresponding to a variety of conditions) are given in Table 3. The value of the product of concentration and speed is quite close, in all cases, to the observed flow found directly from the link discharge information. The fact that the latter quantity was calculated by averaging over a series of network "snapshots" taken at 1-min intervals whereas the average speed was determined by parameters accumulated semicontinuously over the same period may account for some of the minor discrepancies apparent in this table.

TABLE 3 Comparison of Average Network Flow with Product of Average Speed and Concentration for Selected Runs

V[a]	K[b]	KV[c]	Q[d]	Difference[e] (%)
12.21	61.38	749	762	1.7
12.74	61.38	782	792	1.3
11.32	69.30	784	810	3.3
12.64	53.46	676	690	2.1
13.20	45.54	601	618	2.8
12.54	27.72	348	354	1.7
12.87	27.72	357	360	0.8
12.24	35.64	436	438	0.5
12.71	35.64	453	456	0.7
11.19	61.38	687	696	1.3
12.90	19.80	255	258	1.2
11.84	45.54	539	546	1.3
12.32	45.54	561	570	1.6
10.70	69.30	742	750	1.1
9.93	79.20	786	798	1.5
11 30	53.46	604	600	-0.7

[a] Average speed in mph, calculated by dividing total vehicle-miles traveled by total time spent in the system by all vehicles.
[b] Concentration in vehicles per link-mile calculated by dividing the constant number of vehicles on the network by total link-miles. Link-miles are used here instead of lane-miles because all links are identical (2 lanes).
[c] Product of V and K in vehicles per hour.
[d] Average flow in vehicles per hour found from the vehicle discharges for each link. (Compare with column 3.)
[e] Percentage difference between KV and Q.

Two-Fluid Theory of Town Traffic

The results of the simulations are analyzed here from the perspective of the two-fluid representation of traffic in a network. As described earlier, traffic is divided into moving vehicles and stopped vehicles. Thus, how various properties aggregated separately over stopped and moving vehicles vary as a function of increasing network concentration and with respect to each other is examined in the context of idealized simulations.

It should first be noted that the relation given by Equation 1 between the average speed of the moving fluid and the average fraction of vehicles running is predicated on the interactions that occur among moving vehicles. In particular, as the concentration in the network increases, and the average speed decreases (meaning that T, the average trip time per unit distance, increases), the average moving time, T_r (per unit distance), has been observed to increase in real urban street networks. This results from perturbations including short stops to pick up or drop off passengers or goods, pedestrian infringement on the right-of-way, illegal and double parking maneuvers, and other incidents that induce sudden braking or forced lane switching. These sources of turbulence occur primarily along the links rather than at the nodes where most controlled stopping takes place.

In the test network, these sources of intralink friction are virtually absent. For instance, no driveways, parking garages, unsignalized minor streets, buses, or pedestrians have been specified. Furthermore, it is not clear that adequate analytic models of the microscopic aspects of these interactions have been developed to date. This deficiency was acknowledged in earlier studies of NETSIM (11, pp.278-280) where intralink "rare events" were believed to be the primary cause of some discrepancy between simulated results and field observations for a few links in the Washington, D.C., central business district. (This led the model developers to introduce the short and long rare event and blockage features in NETSIM to increase its ability to represent realistic features of urban street networks.) In view of the this, the effect of intralink interactions, which are essential in the description offered by the two-fluid theory, was anticipated to be insignificant in idealized simulations; this is reflected in the results presented later in this section.

A key identity invoked in the derivation of the relationship between T and T_s (Equation 2) in the two-fluid theory is that the mean fraction of time stopped is equal to f_s, the average fraction of vehicles stopped. This identity, which can be proved mathematically for a constant number of vehicles circulating in a closed network (3), could be verified. Over a given observation period (following the stabilization period discussed earlier), the mean fraction of time stopped can be readily obtained from the networkwide cumulative statistics generated by the simulation model. The estimation of f_s is not as straightforward; the arithmetic average of a number of snapshots of the network taken at 1-min intervals during the observation period was used. For each snapshot, vehicles stopped in queue were tallied over all links and divided by the total number of vehicles on the network. Twelve snapshots (between the 8th and 20th min of simulation) were thus taken for each run, with the exception of the longer runs where more snapshots could be taken, and averaged to yield an estimate $\hat{f}_s$ of f_s.

Table 4 gives $\hat{f}_s$ alongside the corresponding mean fraction of time stopped, $E(T/T_s)$, for a selected number of runs from both simulation groups (and mean desired speeds) and for varying concentration levels. The percent difference between $E(T/T_s)$ and $\hat{f}_s$, also shown for each run in Table 4, clearly indicates the close correspondence between the two values in nearly all cases. The observed discrepancy stems of course from the coarse discretization on which $\hat{f}_s$ is based. It is actually rather remarkable that as few as 12 snapshots yield such close estimates of f_s,

$$(1/\tau)\int_{t_o}^{t_o+\tau} f_s(t)dt$$

where $f_s(t)$ is the time-varying fraction of vehicles stopped, and τ the duration of the observation period. Insights into the dynamic behavior of $f_s(t)$ can be obtained by looking at successive

TABLE 4 Comparison of Fraction of Total Time Stopped with Average Fraction of Vehicles Stopped[a] for Selected Runs

Mean Fraction of Time Stopped	$\hat{f}_s$[b]	Difference (%)
0.291	0.298	2.4
0 288	0.295	2.4
0.349	0.352	0.9
0.258	0.269	4.3
0.240	0.242	0.8
0 279	0.297	6.5
0.284	0.274	-3.5
0.292	0.298	2.1
0.295	0.307	4.1
0.351	0.357	1.7
0.353	0.362	2.5
0.260	0.261	0.4
0.313	0.310	-1.0
0.311	0.292	-6.1
0.394	0.405	2.7
0 437	0.443	1.4
0.341	0.350	2.6

[a] Estimated from discrete snapshots.
[b] Based on 1-min snapshots.

snapshots, obtained at 1-min intervals, for one or more runs. Figure 7 shows such snapshots for two selected runs. The bottom line corresponds to a group 1 run (35-mph mean desired speed) with a network concentration of 30.69, and the top line corresponds to a group 2 run (35-mph mean desired speed) and concentration of 39.60. For both runs, the variation is rather substantial, which is typical of all the simulations performed. Variation of average fraction of vehicles stopped as a fraction of network concentration is discussed later in this section.

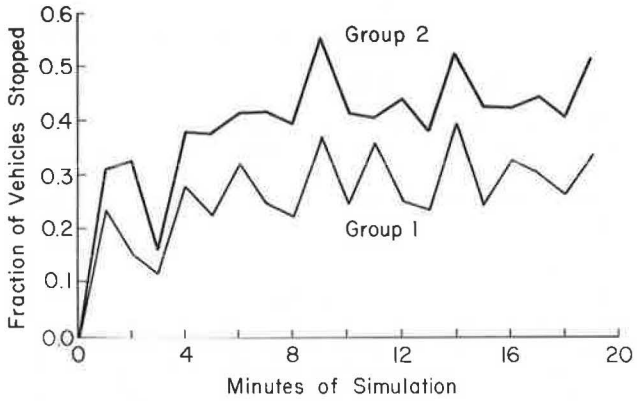

FIGURE 7 Instantaneous fraction of vehicles stopped evaluated at successive network snapshots for two selected runs.

The variation of T, T_s, and T_r as a function of network concentration, K, while network control features and traffic characteristics are kept fixed, is examined next. Group 2 simulation runs with mean desired speed of 35 mph are considered for this purpose. Table 5 gives a summary of the values of T, T_r, and T_s that correspond to concentrations of up to 75 vehicles per lane-mile; also given are the ratios T_r/T and T_s/T. As expected (and seen earlier in the discussion of the K-V relationship), the average trip time per unit distance, T, increases with increasing concentration. It can also be seen from the values of T_s that this increase in T is due overwhelmingly to increasing stopped time; the average running time (per unit distance), T_r, is seen to remain at approximately the same level throughout. This behavior, which does not correspond to that observed in real urban networks, confirms the concerns about the inadequate representation of perturbations and interactions that are an integral aspect of urban street traffic. The almost constant T_r obtained in these runs corresponds to a value of the parameter n (of the two-fluid model), which is not significantly different from zero, indicating the relative lack of sensitivity of T_r to changes in the fraction of vehicles running in the range of concentrations considered in the idealized system. It is, however, conceivable that greater realism could be achieved by specification of random "rare events" (allowed by NETSIM) or other sources of interference; an investigation of these possibilities was beyond the scope of the present exploratory study. Further thoughts on this matter are offered in the next section.

Table 5 also allows examination of the variation of f_s (which is identical to T_s/T) as a function of network concentration. An analytical relationship between f_s and K, proposed by Herman and Prigogine (1) as an extension of the two-fluid model, has been presented (Equation 3). The general trend predicted by Equation 3 is present in the results of the simulations whereby f_s increases nonlinearly with increasing concentration; this trend is shown in Figure 8. It can also be seen in Figure 8 that the fraction of vehicles stopped tends to level off and not fall below a minimum threshold at lower concentrations. A plausible explanation is that, over any meaningful observation period, it is inevitable that a number of stoppages will occur due to the nature of the traffic control system governing the network used in the simulations. In other words, it is virtually impossible to circulate in a network of this type for 12 min within some fraction of the vehicles stopping at some of the frequently encountered signals.

A least-squares estimation of the parameters p and K_m in Equation 3 yielded the values 0.589 and 156.0 vehicles per lane-mile, respectively. Note that these estimates are for K in the range of 15 to 75 vehicles per lane-mile. The corresponding R^2 was equal to 0.988. It is interesting to note here that the magnitude of K_m is consistent with its interpretation as the concentration at which the network "jams." A partial simulation run with an intended K of 150 vehicles per lane-mile showed extreme congestion levels with prevailing spillbacks at most intersections, which effectively delayed the complete loading of the vehicles onto the network by as much as 20 min after the last vehicle was emitted from the source nodes. (Computational cost considerations prevented the pursuit of the matter further at this stage with such unrealistically high concentration levels.)

TABLE 5 Average Trip Time, Stop Time, and Running Time Characteristics for Group 2 Runs[a] Under Varying Network Concentration Levels

Concentration (veh/lane-mile)	Trip Time[b] (T)	Running Time[b] (T_r)	Stop Time[b] (T_s)	T_r/T	T_s/T
1.98	4.41	3.34	1.07	0.758	0.242
2.97	4.38	3.30	1.08	0.754	0.246
13.86	4.66	3.34	1.33	0.716	0.284
17.82	4.72	3.33	1.39	0.705	0.295
22.77	4.87	3.35	1.52	0.689	0.311
34.65	5.61	3.40	2.21	0.606	0.394
39.60	6.04	3.40	2.64	0.563	0.437
48.51	6.86	3.41	3.44	0.498	0.502
56.43	7.80	3.41	4.39	0.437	0.563
65.34	8.62	3.39	5.24	0.393	0.607
74.25	9.68	3.37	6.31	0.349	0.651

[a] 35 mph mean desired speed.
[b] T, T_r, and T_s are averages (over time and over vehicles) expessed in minutes per mile.

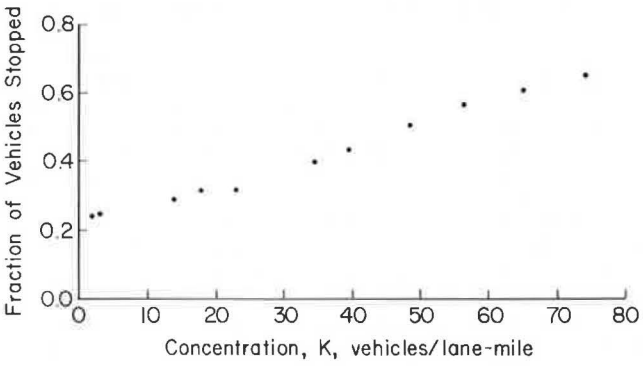

FIGURE 8 Average fraction of vehicles stopped versus network concentration, group 2 runs (35 mph mean desired speed).

SUMMARY AND ASSESSMENT

An exploratory study designed to assess the usefulness of a simulation-based approach to support the investigation of network-level macroscopic traffic flow relationships has been discussed. The NETSIM microscopic network traffic simulation model was used in conjunction with an idealized system consisting of an isolated CBD-like rectangular grid network operating under various combinations of traffic control schemes and characteristics. The results were analyzed with respect to (a) network traffic flow theory, (b) the two-fluid theory of town traffic, and (c) flow distribution on network components.

The analysis of flow distribution on network components was concerned primarily with the dynamic behavior of the relative concentrations and flows on boundary links and interior links, respectively. Useful insights were gained regarding the general stabilization of the respective fractions of vehicles and flows on boundary and interior links after an initial period. This provided the basis for defining an appropriate observation period over which average traffic descriptors, used in other parts of this study, were calculated.

Two principal network traffic flow theoretic relationships were addressed. Average network speed was found to decrease as a function of increasing network concentration, as anticipated, with an overall trend that is not unlike that observed for arterials. This trend was also explored under varying signal timing schemes and traffic characteristics. The second relationship addressed was $Q = KV$, which is fundamental for arterials but unverified at the network level. Simulations seemed to indicate that, for properly defined averages of the three quantities, $Q = KV$ could be expected to hold.

The analysis of the results from the perspective of the two-fluid theory of town traffic verified the identity between the average fraction of vehicles stopped and the mean fraction of time stopped for a fixed number of vehicles circulating in a closed network over the same observation period. The dynamic behavior of the instantaneous fraction of vehicles stopped was also examined. In addition, the variation of the average fraction of vehicles stopped as a function of network concentration was studied and seemed to indicate that a proposed extension of the two-fluid model (1) holds rather well over a middle range of concentrations. On the other hand, the idealized simulation conditions apparently did not generate the interactions among moving vehicles that constitute an essential feature of real urban traffic systems operations and that, as such, are critical to the description encapsulated by the two-fluid theory.

It is essential to re-emphasize here the exploratory nature of the research described. It is evident that a number of probably severe limitations are present in the preliminary results. The list of these limitations includes the highly idealized nature of the system and its operating conditions, the well-known fact that a simulation model is only an abstraction of the real world, and many others ranging from specifics of the execution to the restricted scope of the results and associated conclusions. It is nevertheless believed that such exploratory studies yield useful insights into the behavior of traffic systems under a variety of conditions that cannot be easily achieved in the real world. Such studies can provide a useful complement to observational studies of network-level traffic phenomena, which remain the cornerstone of a scientific approach to the development of a network traffic flow theory. By raising questions and probing some possible answers, simulation-based studies can suggest to the analyst important directions for both theoretical and observationally based advances.

A number of avenues exist for further effort in this general area of investigation. Some of the more immediate ones include the assessment of how NETSIM could be used to adequately describe the interactions among moving vehicles or intralink phenomena that are fundamental in real urban street systems. It was mentioned earlier that the introduction of short- and long-term rare events and blockages, in addition to heavy vehicles, pedestrian interference, driveways, and parking maneuvers, is likely to improve the realism of this representation. However, more fundamental modifications in the car-following and lane-switching procedures embedded in NETSIM may be required. A related possibility exists for using some of the recent empirical results obtained in conjunction with the two-fluid theory whereby one or two test vehicles circulating in a network can yield sufficient information for characterizing the quality of traffic service in an urban network (3,4). This relatively easily acquired information could provide the basis for calibrating a simulation model like NETSIM, particularly with respect to difficult-to-model intralink interactions.

ACKNOWLEDGMENTS

Partial support for the research on which this paper is based was provided by a grant from the Bureau of Engineering Research at the University of Texas (to H. Mahmassani), as well as by U.S. Department of Transportation grant DOT DTRS 5781-P-81539. The assistance of Patricia A. Best, undergraduate research assistant at the University of Texas at Austin, in the processing of the tons of computer output and in the graphic presentation is particularly appreciated. The authors remain, of course, solely responsible for the contents of this paper.

REFERENCES

1. R. Herman and I. Prigogine. A Two-Fluid Approach to Town Traffic. Science, Vol. 204, 1979, pp. 148-151.
2. M.-F. Chang and R. Herman. Trip Time Versus Stop Time and Fuel Consumption Characteristics in Cities. Transportation Science, Vol. 15, 1981, pp. 183-209.
3. S. Ardekani and R. Herman. Quality of Traffic Service. Research Report 304-1. Center for Transportation Research, University of Texas, Austin, 1982.
4. R. Herman and S. Ardekani. Characterizing Traffic Conditions in Urban Areas. Smeed Memorial Lecture. University College, London, England, May 1983.
5. D.L. Gerlough and M.J. Huber. Traffic Flow Theory: A Monograph. TRB Special Report 165. TRB, National Research Council, Washington, D.C., 1975.
6. D. Gazis, ed. Traffic Science. Wiley, New York, 1974.
7. Highway Capacity Manual 1965. HRB Special Report 87, HRB, National Research Council, Washington D.C., 1965, 397 pp.
8. I. Prigogine and R. Herman. Kinetic Theory of Vehicular Traffic. American Elsevier, New York, 1971.
9. Traffic Network Analysis with NETSIM--A User

Guide. Implementation Package FHWA-IP-80-3. FHWA, U.S. Department of Transportation, 1980.
10. Peak, Marwick, Mitchell, and Co. Network Flow Simulation for Urban Traffic Control System: Phase II, Volumes 1-5. FHWA, U.S. Department of Transportation, 1973.
11. Peat, Marwick, Mitchell, and Co. and General Applied Science Laboratories, Inc. Network Flow Simulation for Urban Traffic Control System. Final Report. FHWA, U.S. Department of Transportation, 1971.

Publication of this paper sponsored by Committee on Traffic Flow Theory and Characteristics.

Another Look at Storage Requirements for Bank Drive-In Facilities

JOHN L. BALLARD, JOHN G. GOBLE, RICHARD J. HADEN, and PATRICK T. McCOY

ABSTRACT

Observations of the operation and performance of bank drive-in facilities in Lincoln, Nebraska, indicated that current storage requirements for these facilities were excessive. The objective of this research was to determine why these theoretically and empirically developed requirements were excessive and to develop more reasonable storage requirements. Arrival and service-time data collected at bank drive-in facilities were analyzed. It was determined that the arrivals were Poisson. But, contrary to the usually employed queuing theory assumptions of negative exponential serving times, which had been used to develop previous storage requirements, the service-time distributions were found to be gamma distributions with shape parameters between 2.75 and 5.00. Because of the intractability of using queuing theory with gamma service-time distributions, simulation models of single-queue and multiple-queue, multiple-channel queuing systems typical of bank drive-in facilities were developed and validated. The models were then used to determine more appropriate storage requirements.

Before April 1981 the storage requirements for bank drive-in facilities imposed by the city of Lincoln, Nebraska, were those given in Table 1. These requirements were developed from a review of the literature, primarily papers written by Woods and Messer (1) and Scifres (2), and the results of field studies conducted by the city in 1974, which in general confirmed the findings presented in the literature. These requirements were generally accepted as reasonable for several years. Beginning in 1980 they were challenged for requiring too much storage, and the need for updated studies became apparent.

TABLE 1 City of Lincoln, Nebraska, Drive-in Bank Storage Requirements Before April 1981

No. of Windows	Minimum Storage Required[a,b] (vehicles)
1	7
2	14
3	21
4	28
5	30
6	30

[a] In addition to the service position.
[b] 22 ft per vehicle required in storage lanes.

The need for updated studies resulted primarily from major changes in the banking industry in Lincoln. Among these changes were

1. A sharp increase in the number of drive-in facilities available, spreading the business around and reducing peaking at any one facility.
2. The introduction of 24-hour electronic teller machines at sales points such as grocery stores provided a new convenience for customers. This raised the customers' expectations and reduced their tolerance of delay.
3. There was an increased trend toward staggered payrolls among major employers, which reduced peaking characteristics for deposits and withdrawals.

Consequently, in early 1981, the city conducted studies of traffic operations at drive-in banking facilities to determine the reasonableness of its storage requirements. A total of 1,142 transactions were observed during which the average traffic intensity was 0.89. However, the maximum queue length observed in any one storage lane was only five vehicles, and it existed for only 18 sec. Otherwise, the maximum queue length was four vehicles. The average transaction time observed was 2.12 min, which is considerably lower than the average service times often assumed in design guidelines (1,2). In addi-